
Journal of Computational Neuroscience 15, 247–269, 2003

Visual Responses of Crayfish Ocular Motoneurons: An Information Theoretical Analysis

C.S. MILLER
Department of Biochemistry and Cell Biology, Rice University, Houston, TX 77005, USA

D.H. JOHNSON
Department of Electrical and Computer Engineering, Rice University, Houston, TX 77005, USA

J.P. SCHROETER, L. MYINT AND R.M. GLANTZ
Department of Biochemistry and Cell Biology, Rice University, Houston, TX 77005, USA
rmg@bioc.rice.edu

Received January 14, 2003; Revised May 12, 2003; Accepted May 13, 2003

Action Editor: John P. Miller

Abstract. Motoneuron responses were elicited by global visual motion and stepwise displacements of an illuminated stripe. Stimulus protocols were identical to those used in previous behavioral studies of compensatory eyestalk reflexes. The firing rates and directional selectivity of the motoneuron responses were measured with respect to four stimulus dimensions (spatial frequency, contrast, angular displacement and velocity). The directional selectivity of the motoneuron response was correlated to the previously measured gain of the reflex for each stimulus dimension. The information theoretical analysis is based upon Kullback-Leibler (K-L) distances which measure the dissimilarity of responses to different stimuli. K-L distances for single neurons are strongly influenced by the mean rate difference of the responses to any pair of stimuli. Because of redundancy, the joint K-L distances of pairs of neurons were less than the sum of the K-L distances of the individual neurons. Furthermore, the joint K-L distances were only weakly influenced by correlations among coactivated neurons. For most of the stimulus dimensions, the K-L distances of single motoneurons were not sufficient to account for the stimulus discriminations exhibited by the eyestalk reflex which typically required the summed output of 2 to 5 motoneurons. Thus the behaviorally relevant information is encoded in the motoneuron ensemble. The minimum time required to discriminate the direction of motion (the encoding window) for a single motoneuron is about 380 to 480 ms (including a 175 ms response latency) for stepwise displacements and up to 1.0 s for global motion. During this period a motoneuron fires 2 to 3 impulses.

Keywords: optomotor, Kullback-Leibler, rate code, correlation, encoding window, reflex, vision

Introduction

Optomotor neurons form the final stage of the neural pathways of compensatory ocular reflexes. These reflexes rotate the eyestalk so as to stabilize the retinal image during body rotation. The motoneurons are under the control of sensory pathways (e.g., visual neurons, statocysts) and their activity is closely related to optomotor behavior. Because the motoneuron discharge is both a representation of sensory information

and an instruction for behavior it is particularly useful for examining the information coding strategies in the nervous system.

In this study we examine the relationship between the activity of motoneurons and the visually elicited pitch compensation reflex (Miller et al., 2002). The motoneurons are initially considered in terms of the stimulus-dependence of the mean rate and directional selectivity for variations across several stimulus dimensions. The same data are also analyzed with an information theoretic metric which estimates how well any two visual stimuli are discriminated by an optimal processor of the responses. The motoneuron responses are considered both as single cells or in small ensembles. All of the above aspects of the motoneuron responses are compared to related functions of the eyestalk reflex.

Previous studies of optomotor neurons in crabs (Burrows and Horridge, 1968; Silvey and Sandeman, 1976), crayfish (Wiersma and Oberjat, 1968; Mellon and Lorton, 1977; Hisada and Higuchi, 1973) and lobsters (York and Wiersma, 1975) indicate that the functional properties of the motoneurons are qualitatively related to the operating characteristics of optomotor reflexes. Each of the above groups of decapods, exhibits a compensatory reflex for rotation of the animal about the transverse axis. A subpopulation of the optomotor neurons and the pitch compensation reflex are driven by comparable perturbations in the same sensory modalities (e.g. vision, and the equilibrium sense associated with the statocysts) (Wiersma and Oberjat, 1968; Mellon and Lorton, 1977; York and Wiersma, 1975; Neil et al., 1983; Miller et al., 2002). Because the eyestalk is supported by a suspensory ligament, it is likely that several muscles and subsets of motoneurons participate in any given eyestalk rotation. The neuromuscular subsystems that underlie pitch compensation appear to have a relatively simple organization in crayfish (Robinson and Nunnemacher, 1966; Hisada and Higuchi, 1977; Mellon, 1977). The principle effectors are a pair of antagonistic muscles each innervated by 3 motoneurons (Mellon, 1977).

Methods

Physiological Procedures

The preparation of the crayfish, *Procambarus clarkii*, was similar to that of Wiersma and Oberjat (1968). At least two days before an experiment the chelipeds were removed by autotomy (self-amputation) and the rostrum was cut away to expose the basal joints of the eyestalks. The eyestalks were fixed in their sockets with cyanoacrylate adhesive (Superglue). The wounds were allowed to heal for 48 hours before recording. At the time of recording two fine holes were drilled in the cuticle of the eyestalk and a third in the cephalothoracic carapace for a reference electrode. The crayfish was mounted in the recording apparatus that contained a concave disc of plexiglass (15 mm in diameter and 5.0 mm thick) attached to a steel rod. The concave surface of the plexiglass was fixed to the dorsal surface of the carapace with cyanoacrylate. This procedure fixed the position of the animal without creating visual obstacles in the dorsal half of visual space. The ventral half of the animal including the gill chambers was wrapped in moist tissue to prevent dessication.

The recording electrodes were made of 0.25 mm tungsten rod, etched to a 2.0–5.0 μm tip diameter and covered with an epoxy based insulator except at the tip. The electrode signals were led to an A-M Systems differential A.C. amplifier and the amplifier output was led to an oscilloscope, audio monitor and a data acquisition system (see below).

The two recording electrodes were inserted through the previously described holes in the eyestalk cuticle and adjusted until the optomotor neuron impulses were detected on the audio monitor. The optomotor neurons of the pitch and roll compensation systems are identified by three functional criteria (Wiersma and Oberjat, 1968; Mellon and Lorton, 1977): (i) Each of the motoneurons has a distinct visual receptive field. Thus in the pitch compensation system, the head-down (HD) motoneurons are excited by illumination of the dorsoposterior quadrant of visual space and inhibited by illumination of the dorso-anterior quadrant. For the head-up (HU) motoneurons it is just the reverse. The side-up motoneurons (SU) are excited by light to the central pole of the ipsilateral eye and inhibited by light to the central pole of the contralateral eye and *vice versa* for the side-down (SD) motoneurons. (ii) The name of each cell indicates the orientation of the animal *in the dark* that elicits the highest impulse rate derived from statocyst afferents (Wiersma and Oberjat, 1968; Hisada and Higuchi, 1973). Thus rotating the crayfish about its transverse axis so as to pitch the head upwards excites the HU motoneurons while pitching the head downwards excites the HD motoneurons, and similarly for rotations about the longitudinal axis and the SU and SD motoneurons. (iii) Each of the four classes of motoneurons has a distinct directional sensitivity to global visual

motion that would normally be associated with the above body rotations. Thus from a lateral perspective on the right side of the crayfish the HD motoneurons are excited by counter-clockwise rotation of a striped drum and the HU motoneurons are excited by clockwise rotation. The data is derived from recordings of 123 motoneurons from 84 animals.

Stimulus Systems

Two systems were used throughout the study, a mechanical drum and computer generated patterns imaged with an LCD projector. Initially, the mechanical system was used to determine the project's feasibility. By the time the software was operational however, many of the behavioral studies were completed (Miller et al., 2002) and it became necessary to use the mechanical drum in some of the neurophysiological studies to ascertain any differences in the behavior of the neurons associated with the two stimulus systems. The two systems are described in Miller et al. (2002) and only the main features are summarized here.

In the mechanical system, oscillatory motions were produced by the rotation of a plexiglass cylinder (with a stepper motor and eccentric drive) with sine wave gratings attached to the surface. The varied stimulus dimensions included: temporal frequency (0.0019 to 0.5 Hz); spatial frequency (.0055 to 0.36 cycles/deg.); contrast (0.03 to 1.0) and angular displacement ($\pm 10^\circ$ to $\pm 45^\circ$). A linear potentiometer, mounted on the rotation axis, provided signals proportional to the angular rotation of the drum. A panel of flourescent lamps above the drum, provided diffuse illumination of 250 lux inside the drum.

The second system was based upon computer generated patterns and an LCD projector operating at a refresh rate of 60 Hz. The visual patterns consisted of sine wave gratings or single square wave stripes. The intensities and geometry of the generated patterns were software adjusted to compensate for the geometrical distortions (over 140° of visual space) associated with projection onto the cylinder. Motion of the pattern could be selected as a semi-sinusoidal oscillation mimicking the drum rotation of the first apparatus, as a constant angular velocity oscillation, or as a stepwise displacement. The stimulus dimensions were software adjustable over a temporal frequency of 0 to 2.2 Hz; spatial frequency 0 to 0.18 cycles/deg.; contrast 0.04 to 1.0 and angular displacement 0 to ± 70 degrees. Trigger and timing pulses encoding motion direction and pattern position were generated at the computer's serial port. The light intensity of the projector was controlled with software and filters to produce an irradiance in the drum of about 250 lux (similar to the irradiance in the mechanical system) across a homogeneous white field. When the digital system reproduced stimulus conditions associated with the mechanical drum, the resulting optomotor response data were similar.

Step responses were elicited by a single computer-generated stripe which traversed the dorsal visual field. The displacements varied from $\pm 2^\circ$ to $\pm 40^\circ$. In preliminary experiments we tried a number of protocols and found that the optimal stimuli were small displacements across the center of the dorsal visual field.

Data Acquisition

The optomotor responses, the stimulus signal and the calibration signals were digitized with an A/D converter (National Instruments—E series) at a sample rate of 20 KHz under the control of programs written in the LabView (National Instruments, Austin TX) Graphical Language. Comparable digitized recordings were also obtained with a Biologic DRA-400 A/D converter coupled to a Pioneer CD recorder. A third system was used where rapid analysis was required. If the signal to noise ratio was sufficiently high (>5:1) impulses could be detected with a Bak (Germantown Md.) Dual Window Discriminator and event times digitized with a Data Translation 2801 A/D board and Pentium computer with software written in-house. These data could be rapidly converted to poststimulus time histograms (PSTs) to aid in cell classification.

Spike Sorting

In about half of the experiments one or both of the electrodes contained signals from at least two cells (as in Fig. 1A) that were easily separable off-line. When the signal/noise ratio was high (e.g. >5:1) it was sufficient to apply a threshold to the record, examine the suprathreshold impulses (as in Fig. 1B) and determine the event times by comparing each impulse to a unique set of three voltage windows each at a particular time relative to the threshold crossing time. The spike times were then stored as event times relative to the start of each stimulus cycle and with a resolution of 1.0 ms.

When the signal to noise ratio was less than 5:1 the spikes were sorted with a MATLAB (The Mathworks, Natick, MA) clustering routine (MClust, A.D.

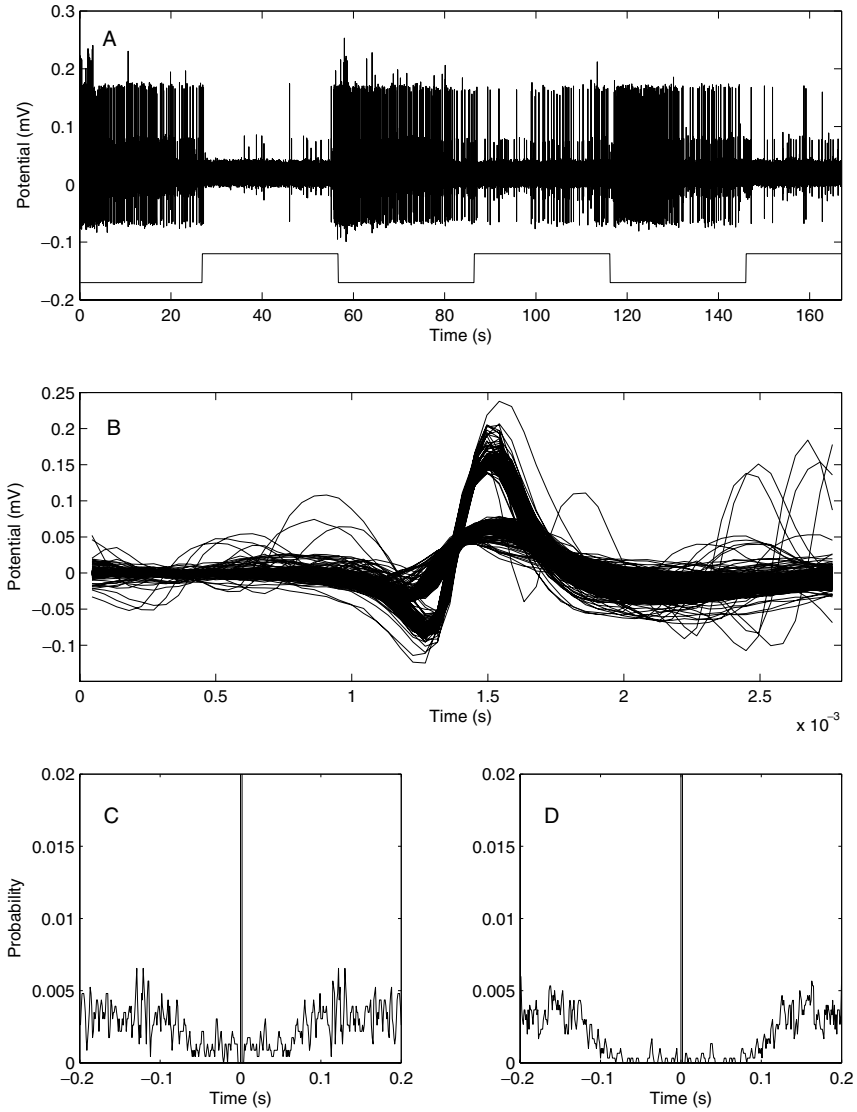

Figure 1. Separation of spikes recorded on the same electrode. (A) Two HD motoneurons recorded on the same electrode. Lower trace indicates the forward (upward) and backward movements of a 2.8° illuminated stripe between locations −2° (posterior) and +2° (anterior). (B) A sample of the two impulses detected by a threshold of 0.04 volts. (C and D) Autocorrelograms of the two new neurons shown in panel B. Bin size is 1.0 ms.

Redish). Candidate spikes were generated by threshold crossings. After the software removed the DC offset from these candidate spikes, it saved both the resulting voltage traces and the times associated with each for later sorting. To separate actual spikes from the list of candidate voltage traces, we exploited the geometric effects on spike waveform and electrode position relative to axon location. The impulses from different cells often have different mean waveform parameters (e.g., peak amplitude, peak width, shape). When the values of any two waveform parameters for the entire set of candidate waveforms are plotted against one another, the spikes from any given single cell will form a "cluster" around the mean values of the two features under consideration. If the mean waveforms of two spike trains have sufficiently different features, their clusters will appear in two distinct locations on such a plot. After the user performs this feature-based classification of the spikes into clusters, MClust creates lists of spike times and feature parameters associated with each cluster. Following waveform classification, these lists are saved to ASCII files for subsequent testing and

analysis. More than one cell can occur in a cluster if two neurons with similar waveforms are equidistant from the recording electrode. Thus the data were subjected to a further test. If the times between spikes were less than the refractory period for a neuron (5.0 ms) we rejected the data and the waveform parameters were respecified. This procedure was repeated until the selected impulses were observed to occupy a unique cluster **and** no more than 1.0% of the interspike intervals were less than the refractory period. Estimates of the refractory period were obtained from interval histograms and autocorrelograms (as in Fig. 1C and D) of well separated units or single unit recordings. About 25% of all the provisionally identified cells were rejected on the basis of the above criteria.

Data Analysis

Several features of the impulse trains were computed throughout the study. These included poststimulus time histograms (PSTs), interspike interval histograms, cross-correlation functions and mean and maximum impulse rates during each of the two phases of grating motion. These analyses were carried out in MATLAB using the built-in matrix functions. The PSTs and cross-correlations were computed with binarized spike trains.

The directional selectivity index (DSI) is derived from the difference between the mean impulse rates elicited by motion in the preferred (P) and null (N) directions. DSI = (P − N)/(P + N). The DSI is computed without correction for the background or 'spontaneous' discharge. In one set of experiments, the response to stepwise displacements of an illuminated bar, the directional selectivity and the sensitivity to variations in angular displacement were principally expressed in the peak transient impulse rate rather than the mean rate. In these experiments P and N were taken from the average rate during the interval from 0.1 to 0.2 s post-stimulus onset.

Information Theoretic Analysis

A response here is the number of spikes occurring in each of L bins. We represent a response by the count vector $\mathbf{n} = [n_1, n_2, \ldots, n_{\mathrm{L}}]$. More than one spike can occur in a bin if the bin width is sufficiently large. When we record from two or more neurons simultaneously, the response is now the number of spikes occurring in each neuron in each bin. We describe the population response by $\mathbf{n} = [\mathbf{n}_1, \mathbf{n}_2, \ldots, \mathbf{n}_{\mathrm{L}}]$, where $\mathbf{n}_l = [n_l^{(1)}, \ldots, n_l^{(\mathrm{M})}]$, where $n_l^{(\mathrm{m})}$ is the number of spikes occurring in the mth neuron during bin l. The K-L distance (Cover and Thomas, 1991) depends on the joint probability function $\mathrm{p}(\mathbf{n}; \alpha)$ describing the response. When the two stimulus conditions are α_0, the reference stimulus, and α, some other stimulus, the K-L distance is defined to be

$$D_{1,\ldots L}(\alpha_0, \alpha) = \sum_{\boldsymbol{n}} p(\boldsymbol{n}; \alpha) \log \frac{p(\boldsymbol{n}; \alpha)}{p(\boldsymbol{n}; \alpha_0)} \qquad (1)$$

We chose base-2 logarithm, which means the K-L distance has units of bits. We plot this K-L distance as a function L, which is proportional to time since the stimulus presentation. We plot the results this way because the K-L distance is related to the asymptotic (as the amount of data increases) performance of a system that tries to discriminate between the two stimulus conditions from the responses. Specifically, the false-alarm probability of the optimal discrimination system is approximately proportional to $2^{(-D_{1,\ldots,L(\alpha\ \mathrm{o},\alpha)})}$ (Johnson et al., 2001). Thus, the larger the distance, the easier it is for an optimal discriminator to discern the stimulus change from the two responses, whether they be from a single neuron or from a population. By estimating the distance between a response pair, we can determine how well the neural encoder presents the stimulus features that correspond to those aspects of the stimulus that distinguish the two stimuli. Plotting (1) as a function of $\mathbf{L}$ reveals how the negative logarithm of the discrimination error probability changes with post-stimulus time.

The K-L distance has the so-called additive property: when the responses are statistically independent of the responses in other bins or in other neurons, the K-L distance equals the sum of the component distances (Johnson et al., 2001). In much of our data, the interspike intervals were weakly correlated (correlation coefficient about 0.1). At high firing rates, this correlation increased to about 0.45, making an assumption of bin-to-bin independence suspect. Consequently, we used the Markov dependence formulation (Johnson et al., 2001) which assumes that each bin's response count is statistically dependent on the count occurring in the previous bin. In this case, an additive formula also applies to the distance calculation, albeit a more complicated one.

$$D_{1,\ldots,L}(\alpha_0, \alpha) = D_1(\alpha_0, \alpha) + \sum_{l=2}^{L} D_{l|l-1}(\alpha_0, \alpha) \qquad (2)$$

where $D_{l|l-1}(\alpha_0, \alpha)$ is the K-L distance between the conditional probability functions describing the distribution of responses in bin l given the number of responses in the previous bin $l-1$.

$$D_{l|l-1}(\alpha_0, \alpha) = \sum_{\boldsymbol{n}_{l-1}, \boldsymbol{n}_l} p(\boldsymbol{n}_{l-1}, \boldsymbol{n}_l; \alpha) \log \frac{p(\boldsymbol{n}_l \mid \boldsymbol{n}_{l-1}; \alpha)}{p(\boldsymbol{n}_l \mid \boldsymbol{n}_{l-1}; \alpha_0)} \quad (3)$$

We calculated the K-L distance by substituting estimates of the response probabilities into Eq. (1) and used the Markov dependence simplification of Eq. (2). The computations used bin widths equal to the modal interspike interval of each data set (typically 20 to 25 ms). Although Eq. (2) takes account of the correlation between successive bins, a consideration of longer term ordering requires larger data sets than we had generated and is not considered here. Our simulations suggest that if long-term ordering is present the correct K-L distance may be modestly larger or smaller than that computed with Eq. (2).

Bias and confidence intervals were estimated using the bootstrap algorithm, which estimates statistics of the KL distance estimate by resampling the original data set on a response-by-response basis. At each bin, the resampling provides an estimate of the K-L distance's probability distribution, from which bias and a confidence interval can be inferred. We used the bootstrap-estimated bias to correct the K-L distance estimate and the confidence interval at each bin. Details of how to use bootstrap to remove bias and estimate confidence intervals in K-L distance calculations can be found in Johnson et al. (2001).

The additive property of the K-L distance can be exploited in population studies. Comparing the population K-L distances to the sum of component distances provides a measure of whether the individual responses are statistically independent of each other or not. When statistically dependent, the population K-L distance can be bigger or smaller than the sum of individual distances. The nature of the discrepancy does not indicate whether the population was positively or negatively correlated; a statistically significant discrepancy simply means that the component responses are not statistically independent.

Because the K-L distance defined in Eq. (1) is usually asymmetric in the stimulus parameters (typically $D(\alpha_0, \alpha)$ is not equal to $D(\alpha, \alpha_0)$), we compute the so-called resistor average distance which is symmetric. This distance is computed from the two K-L distances as

$$\frac{1}{R_{1,\ldots,L}(\alpha_0, \alpha)} = \frac{1}{D_{1,\ldots,L}(\alpha_0, \alpha)} + \frac{1}{D_{1,\ldots,L}(\alpha, \alpha_0)} \quad (4)$$

For each one-bit increase in the resistor-average distance, the probability an optimal system cannot discriminate the stimulus based on observing the measured responses decreases by a factor of $1/\sqrt{2}$.

All references to K-L distances in Results are resistor-averaged distances. We frequently compute the *rate* at which the K-L and resistor-average distances accumulate by dividing the total distance by the response's duration measured in seconds. The resulting rate has units of bits/s, and describes how quickly, on the average, the error probability decreases exponentially over time. Note that this quantity is *not* a communications data rate.

We exploit an important theoretical property of the K-L distance. A result known as the Data Processing Theorem (Cover and Thomas, 1991; Johnson et al., 2001) states that the K-L distances (and resistor average distances as well) computed at a system's input must equal or exceed the corresponding distances computed at its output. Thus, the ability to discriminate the stimuli from responses cannot be better when we observe a system's (e.g. the response of a population of neurons) output than when we observe the input. This property is interpreted to mean that a system cannot express more information than contained in its input.

We focus on the K-L distance in this study instead of entropy or mutual information (Theunissen and Miller, 1991, 1995) because of its direct relationship to decoding (i.e. the performance of optimal classifiers). We could have used the more traditional information theoretic measures to discern whether population components are statistically independent (all share the additive property). However, entropy does not obey the Data Processing Theorem and mutual information can be quite difficult to measure (Johnson, 2002). Mutual information requires knowledge of the joint probability function of the input and output of the system being studied. For example, when studying the behavioral responses, the output is eyestalk motion and the input consists of motoneuron input. Because of the mixed discrete-analog nature of the joint probability distribution in this case and the difficulty of the required simultaneous recordings (motoneuron discharge patterns and eyestalk motion would need to be measured

at the same time), the mutual information estimates are quite difficult to obtain.

Results

Motoneuron responses elicited by a trapezoidal stimulus profile as in Fig. 2 exhibit a number of features that were shared by the majority of cells. Following the onset of grating motion in the preferred direction (Fig. 2, $t = 14$ s), there is an abrupt (within 300 ms) acceleration of the motoneuron discharge rate and the higher rate persists for the duration of this motion segment. Superposed on this elevated discharge are oscillations in the impulse rate (e.g. at $t = 18$ and 22 s) that correspond to the passage of the positive phase of the grating through the motoneuron's visual receptive field. These oscillations, which also persist through the null direction phase of motion (e.g. at $t = 6.0$ and 10.0 s), imply that the motoneurons simultaneously respond to the direction of motion of the global stimulus and to local variations in stimulus intensity.

Another common feature of the motoneuron response is that following the cessation of preferred direction motion, the discharge decelerates slowly (Fig. 2, $t = 0$ to 2 s) and may even persist for the first 1 or 2 s of null direction motion. The slow deceleration, compared to the rapid acceleration of the response to preferred direction motion, implies an asymmetry in the control of the impulse rate in the two directions.

Finally, null direction motion is typically associated with a modest discharge. The minimum null-direction rate, typically about 2 to 3 imp/s, was close to the impulse rate in the absence of visual motion.

The Spatial Frequency Response

Variations of the grating spatial frequency (at constant velocity) influence both the firing rate and the DSI. At

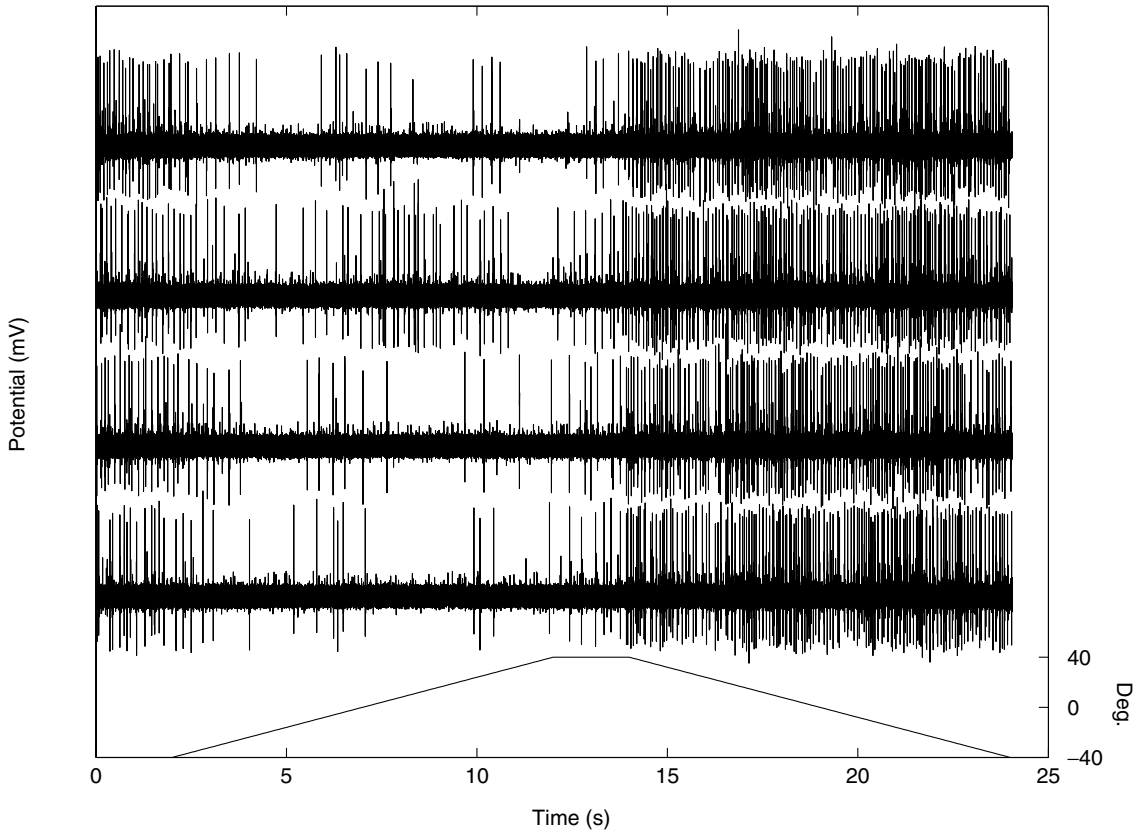

Figure 2. Head down motoneuron responses to the forward and backward motions of a sine wave grating traversing 80° (from −40 to 40°). Four successive responses were displaced vertically. Stimulus position versus time is indicated on the bottom trace with respect to the right-hand ordinate.

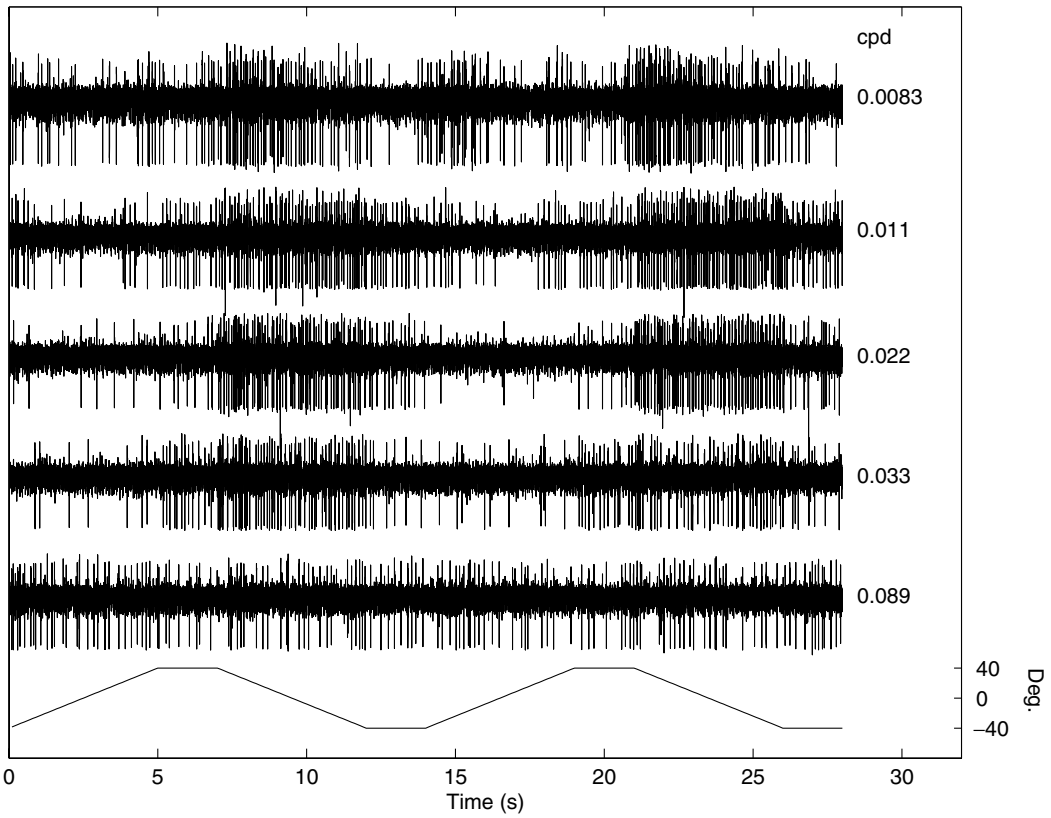

Figure 3. Head down motoneuron responses to the motion of sine wave gratings of varied spatial frequency indicated adjacent to each trace in cycles per degree (cpd). The timing of stimulus motion between −40° (at the origin) and 40° (maximum) is indicated on the bottom trace.

the extremes of the spatial frequency spectrum the firing rates are minimally influenced by stimulus motion and the DSI is close to zero, as in Fig. 3, 0.089 cycles/deg (cpd). This high-frequency cut-off is characterisitc of the whole population (as in Fig. 5A and B) although a few cells do exhibit a significant DSI at 0.089 cpd as shown in Fig. 4A. Maximal impulse rates and DSI occur at spatial frequencies of 0.022 to 0.044 cpd.

PSTs, as in Fig. 4A, reveal both the directional selectivity of the responses to intermediate spatial frequencies and the oscillation in firing rate associated with temporal variations in local irradiance. In this experiment the stimulus velocity was 3.2°/s and each segment of continuous motion covered 80°. Thus, during preferred direction motion, slightly less than one sine wave cycle crossed the field at 0.011 cpd (wavelength (λ) of 90°), just less than 3 cycles at 0.033 cpd (λ of 30°) and 7 cycles at 0.089 cpd (λ of 11°).

Because it is possible these oscillations might arise from the afferent filters associated with motion detection (Egelhaaf et al., 1989) we examined the oscillation period in responses associated with varied grating velocity and at constant spatial frequency. If the oscillations reflect incomplete temporal integration, then the oscillation period should vary inversely with velocity. In 43 measurements from 9 neurons, the absolute difference between the observed oscillation period and that expected from a local intensity detector was 4.9 ± 0.7% (Mean ± SE). Thus we infer that the period of these oscillations is a temporal expression of the grating's spatial frequency. In previous studies (Glantz et al., 1984) we found that the sustaining fibers are functionally connected to these motoneurons. The sustaining fiber response to the same stimuli, though not directional at these velocities, typically exhibits even stronger oscillations as shown in Fig. 4B.

The spatial frequency response of the optomotor system is remarkably consistent with respect to variations in other stimulus parameters (e.g. velocity) as shown in Fig. 5A and B and among the several subsystems that compensate for pitch, roll and yaw (as in Fig. 5C and

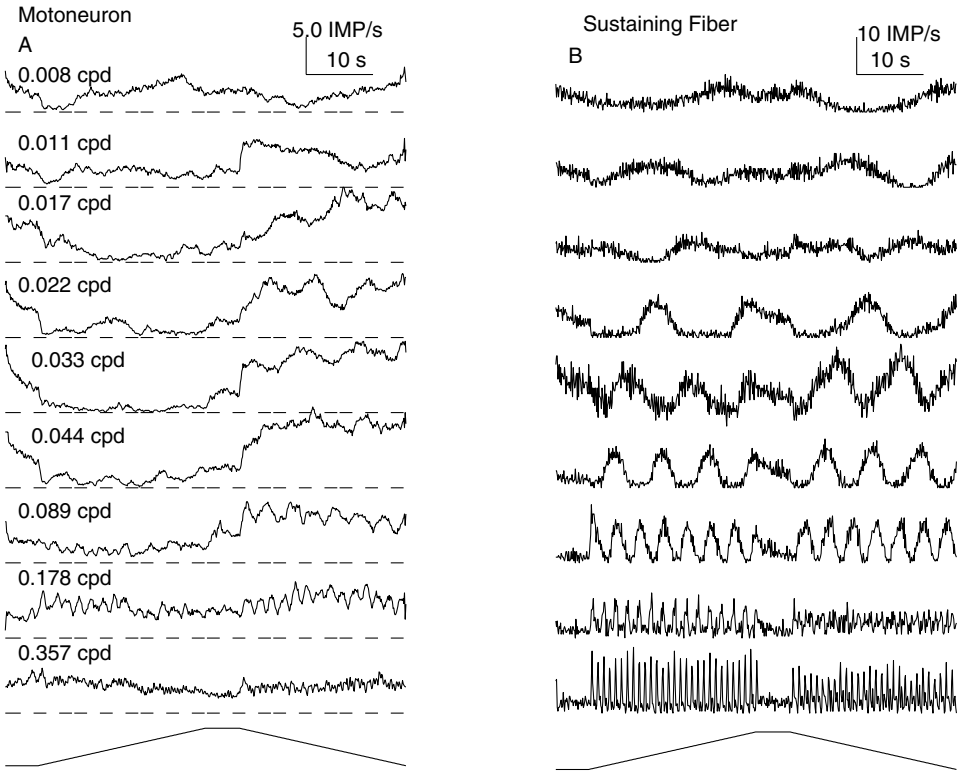

Figure 4. Head-down motoneuron and sustaining fiber firing rates for variations in spatial frequency. (A) Motoneuron responses. Each of the 9 PSTs is the average of 20 stimulus-response cycles with time course indicated on the lowest trace. Stimulus amplitude is 80° (from −40° to 40°) and velocity is 3.2°/s. Bin width is 0.1 s. The broken lines below each motoneuon trace indicate 0 imp/s and the spacing between the broken lines indicates a rate of 10 imp/s. (B) PSTs of responses of a sustaining fiber (038) to the same stimuli as in A. Each PST is the average of 20 responses. Bin width is 0.1 s. The minimum in each histogram is 0 imp/s.

D). The roll and pitch compensation systems have virtually identical DSI-spatial frequency functions but the firing rates of the roll system motoneurons are 20–40% higher than those of the pitch system. The motoneurons of the yaw compensation system (Fig. 5D) exhibit the highest impulse rates by far, and the maximum DSI of the grating-elicited response (*ca.* 0.8) is nearly twice that of the vertical subsystems. In all 3 subsystems the firing rate in the preferred direction is about maximal and that in the null direction is close to the minimum at the optimal spatial frequency determined in behavioral studies (Miller et al., 2002).

Information Theoretic Metrics

An important attribute of the discharge in the motoneuron ensemble is that it contains information about the environment (e.g. the direction of global visual motion). The information theoretic metric we use is the resistor averaged Kullback-Leibler distance which measures how well two stimuli can be discriminated as described in methods. As stimulus-elicited responses proceed over time, the dissimilarity of the responses to two different stimuli increases (as does the K-L distance in Fig. 6). Furthermore, stimuli that are further apart along an effective stimulus dimension will be distinguished by larger K-L distances, as also shown in Fig. 6. Thus two spatial frequencies, 0.033 and 0.022 cpd, are only modestly different to the crayfish optomotor system and the K-L distance distinguishing their responses is 51 bits in 60 s (or 0.83 bits/s) as in Fig. 6B (solid line). Conversely, spatial frequencies 0.033 and 0.0083 cpd are further apart and the K-L distance between their responses, 118 bits (or 1.97 bits/s) implies that the latter pair are 48% ($2^{(1.97-0.83)/2}$) more discriminable than the former. The slopes of the K-L functions in Fig. 6 vary in time in accordance with the

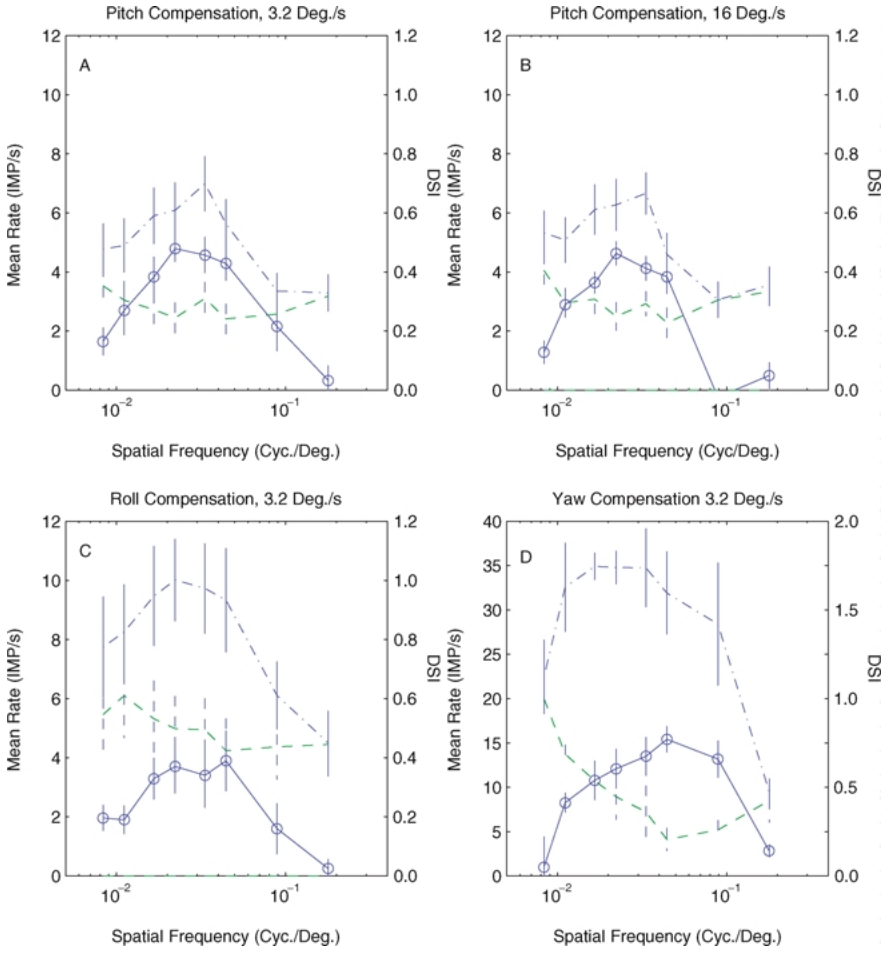

Figure 5. Population mean rates for preferred (dash-dot lines) and null (dashed lines) directions of motion and the DSI (solid lines, open circles) versus spatial frequency. (A) Pitch compensation motoneurons at velocity 3.2°/s, $n = 17$. Vertical bars are ±1.0 S.E. of the means. (B) As in A but velocity is 16°/s, $n = 14$. (C) As in A but for roll compensation motoneurons, $n = 7$. (D) Yaw compensation motoneurons, $n = 4$. Note the change in ordinate scale.

differences between the two compared responses. Thus the interval from 5 to 30 s post-stimulus onset corresponds to the null phase of stimulus motion and the underlying responses are only modestly different (see Fig. 4 for comparison). Consequently, the slope of the K-L function in Fig. 6A is relatively small during this interval. The period from $t = 35$ to 60 s corresponds to the time of preferred direction motion. The responses exhibit larger differences (compare Fig. 4A, 0.033 to 0.008 cpd) and the slope of the K-L function in Fig. 6A is steeper. So long as any difference between the responses occurs over a given time interval the cumulative K-L distance will increase over that time interval. Except where noted, subsequent references to K-L distances refer to the average slope of the K-L distance function during the period of preferred-direction motion with units of bits/s.

Spatial frequency discrimination by motoneurons is related to the difference between the compared stimuli (as in Fig. 7A, solid line) and the discrimination is relatively insensitive to stimulus velocity as shown in Fig. 7A (solid versus broken lines). Increasing the stimulus amplitude however, (from ±10° to ±45°) increases the dissimilarity of the responses to any pair of stimulus spatial frequencies (compare Fig. 7B broken vs solid lines). At ±45°, the K-L distances evolve at a rate that is 10 to 50% greater than at ±10°.

Both absolute impulse rates and the differences in impulse rates make substantial contributions to K-L distances. The horizontal optokinetic (yaw

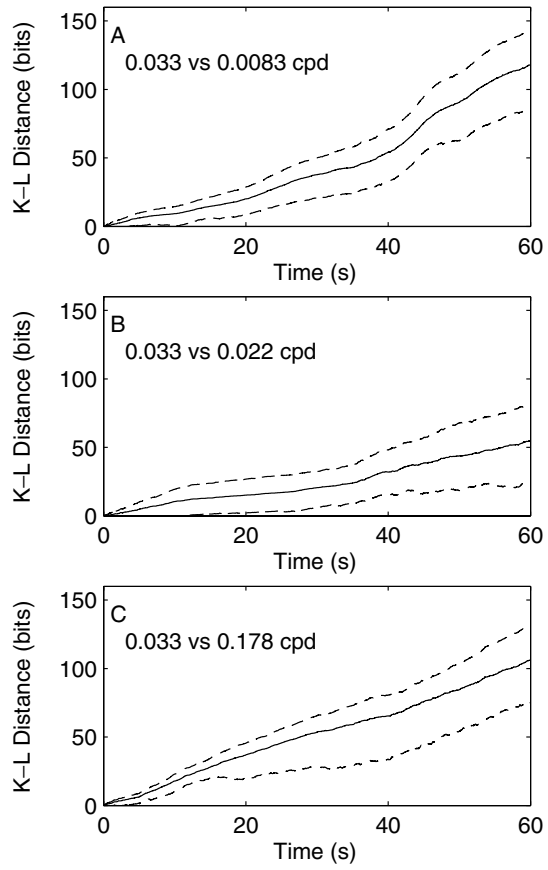

Figure 6. Cumulative K-L distance vs time for comparisons between a response to a reference spatial frequency (0.033 cpd) and responses to three other spatial frequencies. The K-L computations were performed on the same data used to construct the PSTs in Fig. 4A but the bin width was 20 ms. In A–C the solid lines indicate the average K-L distance and the broken lines indicate the ±90% confidence intervals. The horizontal (time) axis corresponds to **L** in Eq. (2).

compensation) motoneurons exhibited both the highest mean rates and the largest rate differences for variations in spatial frequency as shown in Fig. 5D. The impact of impulse rate on K-L distance can be inferred by comparison of the K-L distances in Fig. 7C of optokinetic motoneurons (mean preferred rate about 40 imp/s at spatial frequency reference) to those in Fig. 7B (broken line) for pitch compensation motoneurons (10 imp/s mean rate at spatial frequency reference) under similar stimulus conditions. The comparison indicates that a 4-fold difference in mean rate is typically associated with about a 2-fold difference in the maximum K-L distance.

Because eyestalk rotation reflects the activity of ensembles of motoneurons, it is important to determine how the contributions of coactived cells are added in an information theoretic sense. When two motoneurons are monitored simultaneously, we can determine the K-L distance (for the responses to pairs of spatial frequencies) from the separate cells as in Fig. 7D or we can compute the joint K-L distance evaluated from the simultaneous activity (as in Fig. 7E—solid line). When compared to the sum of two K-L distances taken separately, the joint distance is on average ($n = 269$) about 87% of the sum of the two separate distances. This result implies that there is redundancy in the signals carried by the two motoneurons. The results (as in Fig. 7F) were similar for pairs of synergists, which discharge during the same stimulus phase, and pairs of antagonists, which fire 180° out of phase.

Influence of Correlation on K-L Distance

A well established feature of crustacean motoneurons is that their activity may be coordinated by direct synaptic interactions (Mulloney and Selverston, 1974; Tatton and Sokolove, 1975; Wiens and Gerstein, 1975). Cross-correlations of motoneuron spike trains frequently yielded results consistent with synaptic interactions as shown in Fig. 8A. Excitatory interactions among synergists were the most common and they were always unidirectional. The correlograms indicated that in correlated cells, 5 to 50% of the visually elicited impulses of one motoneuron occurred 2 to 10 ms after an impulse in a synergist. These correlations appear to have only a small influence on the ensemble K-L distances as shown in Fig. 8B and C. For correlated motoneurons, the joint K-L distance (Fig. 8C, ×) was 91.4 ± 1.9% (Mean ± SE, $n = 122$) of the sum of the two K-L distances measured separately. The comparable figure for uncorrelated cells was 82.7 ± 2.3% ($n = 147$) (Fig. 8C, open circles). Although the effect of correlation is only a 10% enhancement of the joint K-L distance, it is highly significant ($p < .005$). It should be noted that the results do not indicate that correlation provides an additional basis for information transmission but rather that correlated ensembles are slightly more efficient at transmitting information than uncorrelated ensembles.

Interspike Interval Distributions

Motoneuron responses are also distinguished by their impulse pattern. The impulse trains of a number of crustacean motoneurons tend to be organized in sequences of brief bursts separated by long interspike intervals

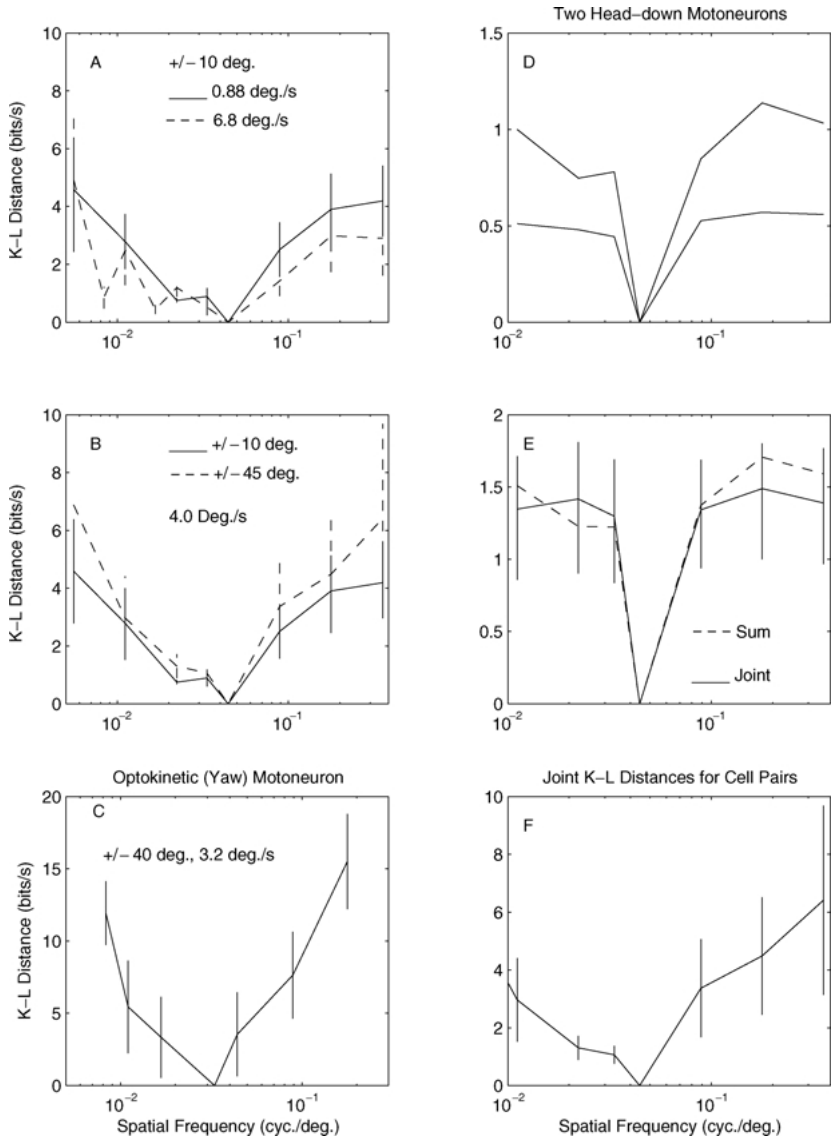

Figure 7. K-L distance versus spatial frequency. (A) K-L distance between responses to each of 8 spatial frequencies compared to the responses at 0.044 cpd and at stimulus amplitude of $\pm 10^{\circ}$. Error bars are $\pm$ S.E. Solid line grating velocity is 0.88°/s, $n = 16$. Broken line velocity is 6.8°/s, $n = 16$. (B) As in A but stimulus amplitude is $\pm 45^{\circ}$ and velocity is 4.0°/s (broken line), $n = 5$. The solid line (presented for comparison) represents the same data as the solid line in panel A (C) K-L distances derived from the response of a single horizontal optokinetic motoneuron with mean rate of 71 imp/s at reference stimulus and indicated stimulus conditions. Vertical bars indicate $\pm$ 90% confidence intervals. (D) Stimulus conditions as in A but for two simultaneously recorded cells. (E) Joint K-L distance of two cells shown in panel D, solid line, compared to the sum of the two K-L distances in panel D (broken lines). The vertical lines indicate the $\pm 90\%$ confidence interval of the joint K-L distances. (F) Joint K-L distances for 29 pairs of simultaneously recorded neurons. The pairs included both synergists and antagonists. Vertical bars are ± 1.0 S.E. Stimulus velocity is 0.88°/s, amplitude is $\pm 10^{\circ}$.

(ISI) (Burrows and Horridge, 1968; Smith, 1974; Kirk and Glantz, 1981). This pattern is optimal for junction potential facilitation (Gillary and Kennedy, 1969) and muscle contraction (Wiersma, 1961). For optomotor neurons we found that the probability of generating short ISI (<20 ms) increased systematically with the firing rate irrespective of the precise stimulus configuration. Nevertheless because the firing rate is generally maximal at the optimal stimulus configuration, many cells exhibit a stimulus-dependent ISI distribution as

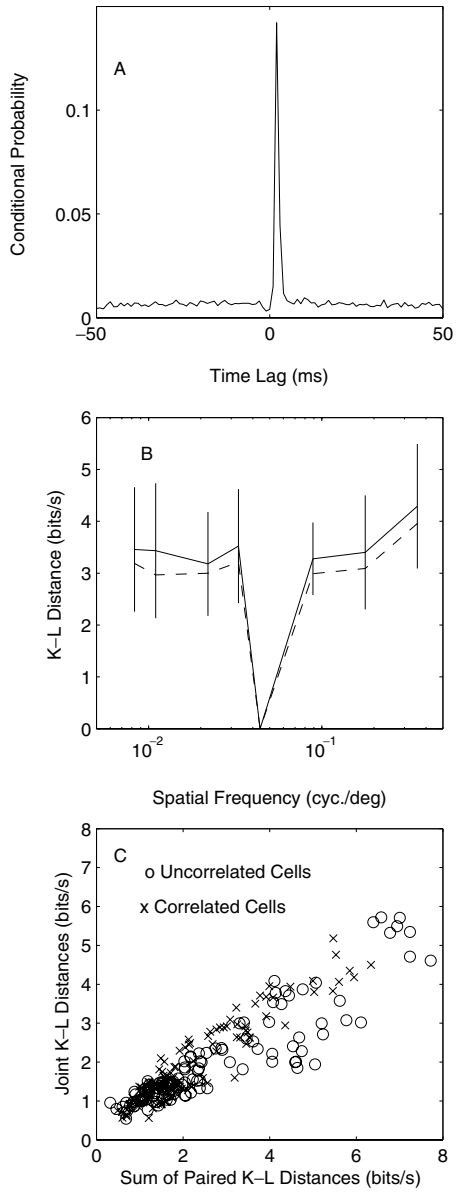

Figure 8. Influence of synaptic interactions between motoneurons on K-L distances. (A) Cross-correlogram of impulses in 2 HD motoneurons. Time lag to peak is 3.0 ms, 8001 reference events, 2595 object events. Peak conditional probability 0.142. Integral of the peak conditional probability is 0.19. About 50% of object train impulses occurred between 2 and 5 ms after a reference train impulse. (B) Joint K-L distance for correlated motoneurons versus spatial frequency (solid line) and sum of separate K-L distances, (broken line). Vertical lines are ±90% confidence intervals of the joint K-L distance. (C) Scatter plot of joint vs. summed K-L distances for 122 measurements on 10 correlated neurons (x) and147 measurements on 15 uncorrelated cells (open circles). The ratio of the joint distance to the sum of the separate distances was 0.827 ± 0.023 (SE) for uncorrelated pairs and 0.914 ± 0.019 (SE) for correlated pairs. The difference is significant ($p < .005$).

shown in Fig. 9A to C. A characteristic feature of these distributions is a mode between 80 and 100 ms and the occurrence of a second mode at short ISI at higher impulse rates. In previous studies (Glantz and Nudelman, 1976) similar variations in other cell types were identified with a regular discharge (and a modal interval weakly sensitive to stimulus conditions) interrupted by doublets or brief bursts for the most effective stimuli. For the cell shown in Fig. 9A–D the probability of generating ISIs less than 20 ms (Fig. 9D, solid line) was correlated to the mean rate ($r = 0.81$). Because the ISI distributions are associated with stimulus-dependent variations in mean rate we computed the correlation between K-L distance and the mean rate difference as shown in Fig. 9E and F. The correlation coefficients for two different velocities was 0.80, suggesting that only 36% ($1–0.8^2$) of the variance in K-L distance is independent of the mean rate difference. When the same analysis is applied to the yaw compensation system (not shown), with larger K-L distances and mean rate differences of up to 60 imp/s, the correlation between the two was 0.94. This result suggests that mean rate is a major determinant of the K-L distance.

The Influence of Stimulus Amplitude

The influence of variations in stimulus amplitude on motoneuron responses were assessed by varying the velocity over a constant time interval or by measuring the impulse rate as the amplitude varied as a function of time (at low velocities). For the combined velocity-amplitude variations the time course of the response is strongly influenced by the velocity as shown in Fig. 10A. These stimuli produced the highest mean rates and DSI for amplitudes of $\pm 2^\circ$ to $\pm 10^\circ$ as shown in Fig. 10C and D. At stimulus velocities less than 1°/s the motoneuron impulse rate (and DSI) increases linearly with displacement for excursions of 25 to 30° (typical) and 45 to 55° in a few cases (as in Fig. 10B). Amplitude differences (associated with velocity variations) produce substantial K-L distances (as in Fig 10E) and the discrimination of other parameters (e.g. spatial frequency and contrast) are enhanced at larger stimulus amplitudes as shown in Table 1.

Contrast and Velocity

Many of the above considerations also apply to motoneuron responsiveness to variations in grating

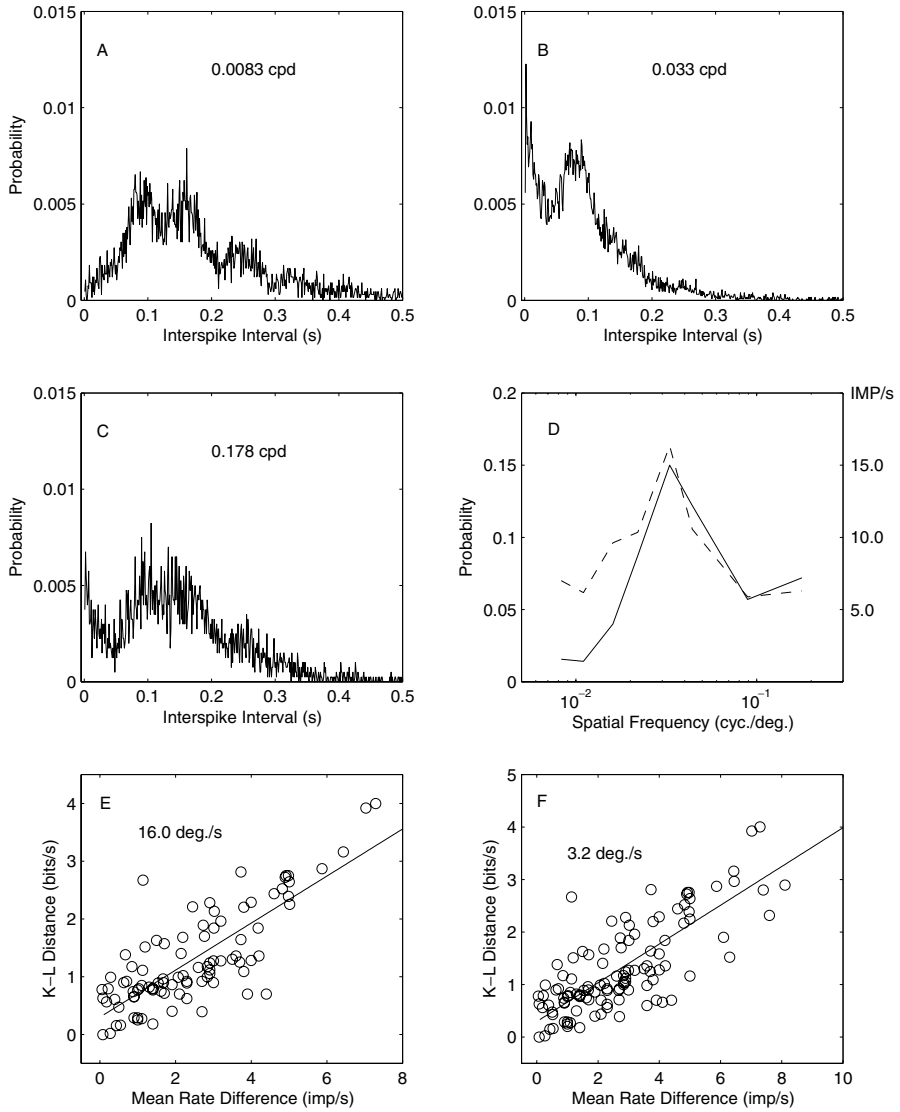

Figure 9. Visual stimuli influence the interspike interval (ISI) distribution. (A–C) ISI distributions of responses to three spatial frequencies indicated in each panel. (D) The probability of brief intervals, 5–20 ms, versus spatial frequency (solid line, left-hand ordinate) compared to the mean rate (broken line, right-hand ordinate). (E) Scatter plot of K-L distance versus the mean rate difference of the compared responses. Velocity 16°/s. The correlation coefficient (r) is 0.80 and the regression slope is 0.41. N is 115 comparisons from 15 motoneurons. (F) As in panel E for velocity of 3.2°/s, 94 response comparisons, 14 neurons. $r = 0.80$ and the regression slope is 0.39.

contrast and velocity. For each dimension the main results are summarized by the DSI functions shown in Fig. 11 (along with behavioral gains (Miller et al., 2002) for the same stimuli) and the information theoretic analysis summarized in Table 1. Variations in grating contrast produced variations in firing rate and DSI for contrasts between 0.02 and 0.2 as in Fig 11C. Contrast variations were only weakly discriminated by motoneuron responses (compared to other variables as shown in Table 1). The velocity profile was measured over the range of 0.35 to 64.0°/s. The DSI as in Fig. 11D was relatively insensitive to velocity variations below 4°/s but declined by 65% at higher velocities.

The Step Response

The pitch and roll compensation systems exhibit both transient and steady-state responses to changes in the

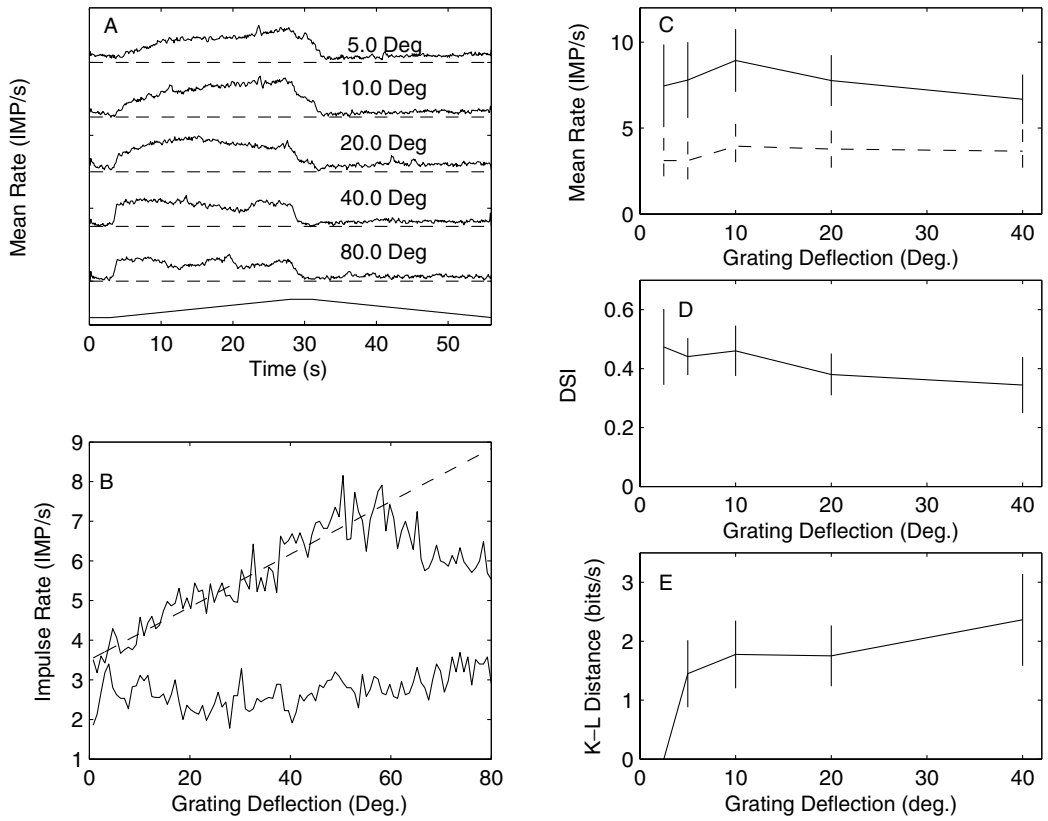

Figure 10. Influence of stimulus amplitude on HU motoneuron rates and DSI. (A) PSTs of responses to covariations in stimulus amplitude (indicated above each PST) and velocity. $N = 20$ per stimulus condition. Bin width is 100 ms. The bottom trace indicates the timing of forward and backward motion. The broken lines between histograms indicate 0 imp/s and they are separated by 15 imp/s along the ordinate. (B) Firing rate (for successive 1.0 s samples) versus grating deflection. Velocity is 0.8°/s. Upper and lower traces are the responses to preferred and null direction motion respectively. The broken line is a linear function with a slope of 0.07 imp/s/deg. Average of 20 responses. (C) Average impulse rates ($n = 5$ cells) during preferred (solid line) and null (broken line) direction motion vs stimulus amplitude. Error bars are 1.0 SE. (D) DSI vs stimulus amplitude, $n = 5$. (E) K-L distance relative to a $\pm$ 2.5° stimulus amplitude as a function of amplitude. Error bars are 1.0 S.E., $n = 5$.

distribution of irradiance over the dorsal half of visual space. For the pitch compensation system the effective stimulus is the gradient of irradiance between the dorso-posterior and dorso-anterior quadrants. For the roll compensation system the effective stimulus is the irradiance difference between the two eyes. In the pitch compensation system, the HU motoneuron is excited by a bar of light deflected from the dorso-posterior to the dorso-anterior quadrant as shown in Fig. 12. The strongest responses are elicited by deflections of $\pm$2.0 to $\pm$15°. Both the time course of the discharge and the mean impulse rate are influenced by the deflection magnitude as shown in Fig. 13. A strong transient response signals the entry of the light bar into the motoneuron's excitatory receptive field, and it typically decays to a plateau phase in less than 1.0 s following the peak. The response is moderately sensitive to the angular displacement of the stimulus as seen in Fig. 13A–D (and the population peak rates in Fig. 14A).

The K-L distances for step displacements (Fig. 13E–G) exhibit a distinct transient phase associated with the peak of the PST. For small displacements ($\pm$2° to $\pm$5°) the transient responses are very similar and this is reflected in the relatively small peak in the K-L function as shown in Fig. 13E. Conversely, when the response to $\pm$2° deflection is compared to that at $\pm$40° (as in Fig. 13G), a substantial difference between the transient responses is reflected in a distinct peak in the K-L function. During this period the cumulative K-L distance (Fig. 13G, broken line, right hand ordinate) increases by 4.0 bits in 80 ms which is about 25 times the average rate of rise. In previous behavioral studies

Table 1. Information theoretic distances for reflex and motoneuron responses.

Stimulus conditions			K-L distance bits/s/octave		K-L distance bits/s (maximum)	
Dimension[a]	Velocity	Amplitude	Mn	Reflex	Mn	Reflex
Spatial frequency	0.88°/s	±10°	1.58 ± 0.50	1.65 ± 0.40	4.50 ± 1.70	1.65 ± 0.40
		JOINT	**2.15 ± 0.45**		**6.33 ± 2.99**	
	3.96°/s	±45°	2.34 ± 0.96	5.30 ± 1.30	6.34 ± 3.16	8.00 ± 1.50
		JOINT	**3.91 ± 1.35**		**9.18 ± 3.62**	
Contrast	3.96°/s	±10°	0.66 ± 0.03	0.55 ± 0.02	1.32 ± 0.32	2.3 ± 0.26
		±45°	1.33 ± 0.10	5.90 ± 1.25	1.92 ± 0.17	20.25 ± 2.68
Amplitude	0.4–8.0°/s	±2° to ±40°	1.32 ± 0.21	7.36 ± 1.05	2.34 ± 0.70	7.36 ± 1.05
Step response	125 to 2500°/s	4.0–80°	2.22 ± 0.23	10.10 ± 3.50	3.01 ± 0.38	12.00 ± 5.7

[a]The standard condition for spatial frequency was 0.033 cycles/deg. and the standard contrast was 1.0. The step response stimulus was a 2.8° stripe.

(Miller et al., 2002), the same stimuli elicited rapid eyestalk rotations and the K-L distance for varied angular displacement was maximal for the first 1.0 s following stimulus onset.

The population averages (Fig. 14A and B) indicate that for the pitch compensation system, the highest impulse rates and DSI occur for deflections of ±2.0 to ±10°, and the DSI function is correlated to the angular deflection of the eyestalk (Fig. 14B, broken line) for the same stimuli. The response profile of the roll compensation system, Fig. 14C, appears similar but the DSI (not shown) increased with displacement. This increase is due to the decline of the firing rate for null direction motion exceeding an amplitude of 20° (as shown in Fig 14C). The responses of the two subsystems also differed in their sensitivity to the width of the stimulus stripe (not shown). The pitch compensation system exhibited maximum DSI for a 2.8° stripe while the roll system was optimally excited by a 30° stripe.

As noted above the K-L distances for eyestalk rotation were most sensitive to angular deflection during the first 1.0 s of the response. The K-L distances of a population of motoneuron responses for varied displacements were evaluated over this same interval as shown in Fig. 14D. The K-L function indicates that large differences in displacement (±2.5° compared to ±40°) are discriminated about twice as well as small differences.

Comparison of Motoneuron and Reflex Responses

We considered three possible aspects of the motoneuron response for comparison to the parametric measurements of reflex gain. These included (i) the impulse rate during the preferred direction of motion; (ii) the difference in rates during preferred and null directions of motion; and (iii) the DSI. The rate during the preferred direction was a poor predictor of reflex gain because it ignores the relative excitation of the antagonist muscles which contributes to the gain of the reflex. In a few instances, the impulse rate in the null motion direction was nearly independent of variations in a stimulus parameter but this was not generally the case. The difference between preferred and null impulse rates and the DSI produced similar correlations to reflex gain. The DSI of pitch compensation motoneurons is compared to the gain of the pitch compensation reflex for 4 stimulus dimensions in Fig. 11. Although the functions differ in numerous respects the DSI and reflex gain are correlated for all stimulus dimensions. The strongest associations were for the spatial frequency and stimulus amplitude data which yielded linear correlation coefficients of 0.91 and 0.94 respectively. There is a consistent disparity between the DSI and gain. When the DSI declines to less than 0.25 there is a disproportionate decline in gain. This disparity is observed at low spatial frequencies, at low contrast and at high stimulus velocities (as in Fig. 11A, C and D respectively). It is possible that this result implies a threshold DSI or preferred direction impulse rate for reflex action.

Discussion

The results indicate that the optomotor neurons are responsive to variations along several stimulus dimensions and the stimulus dependence of the directional

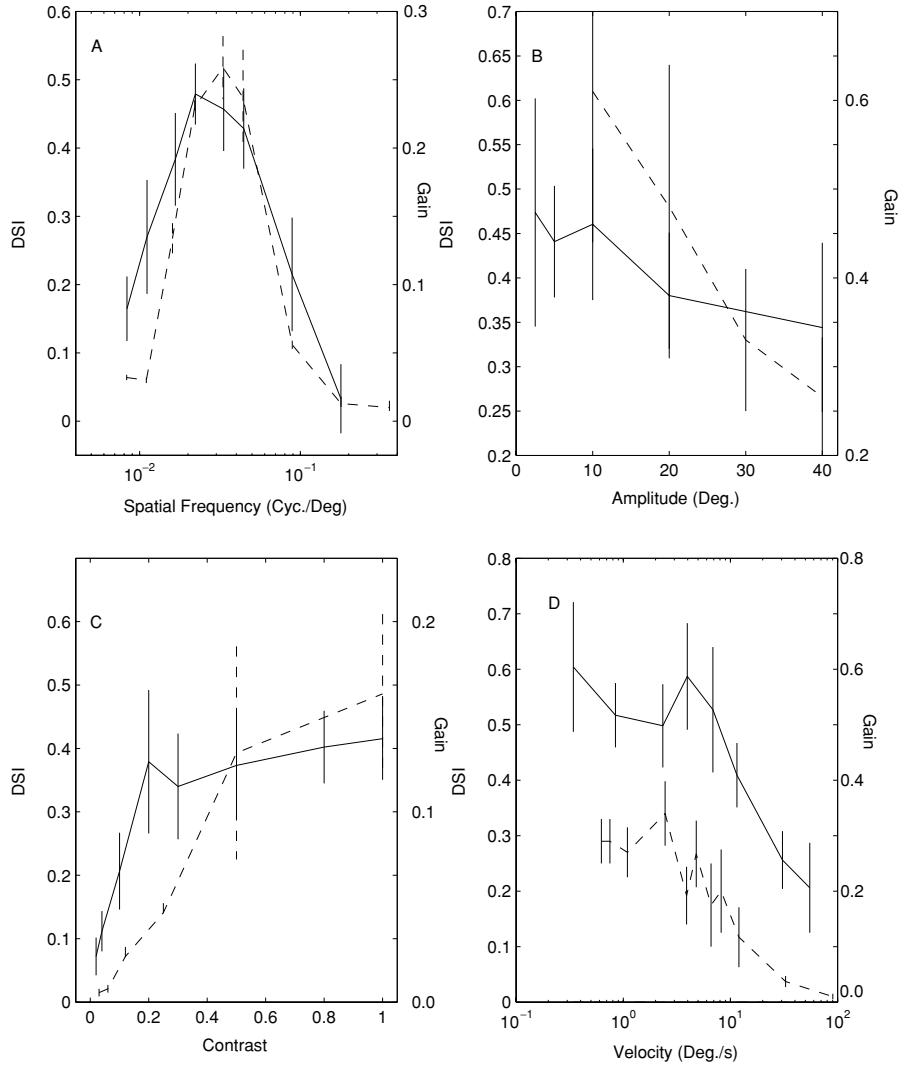

Figure 11. Comparison of motoneuron DSIs (solid line, left hand ordinate) and gain of eyestalk rotation (broken lines, right hand ordinate) for 4 stimulus dimensions. (A) Spatial frequency—DSI and eyestalk gain. Linear correlation coefficient, $r = 0.91$. (B) Stimulus amplitude, $r = 0.94$. (C) Contrast, $r = 0.81$. (D) Grating velocity, $r = 0.87$.

response (i.e. the DSI) is generally similar to that of the gain of the optomotor reflex. These results extend and further quantify previous findings (Wiersma and Oberjat, 1968; Hisada and Higuchi, 1973; Mellon and Lorton, 1977). Motoneurons also exhibit transient responses to the stepwise motion of an illuminated stripe when it enters the excitatory receptive field. The DSI of the transient response for step displacements is correlated to the transient eyestalk rotation described in Miller et al. (2002).

These studies address several issues at the intersection of sensory neuron information coding and behavior. These include the relevance of particular neurons to a specific behavior (deCharms and Zador, 2000), the linearity or nonlinearity of the encoding functions, the size of the encoding ensemble and the temporal window that contains the ensemble message (Theunissen and Miller, 1995).

The anatomical organization of the system (Mellon, 1977) makes it likely that the stimulus-elicited activity of the optomotor neurons is generally relevant to the behavioral response, eye rotation. Because the eyestalk is supported by a suspensory ligament, eyestalk position reflects the coordinated action of several

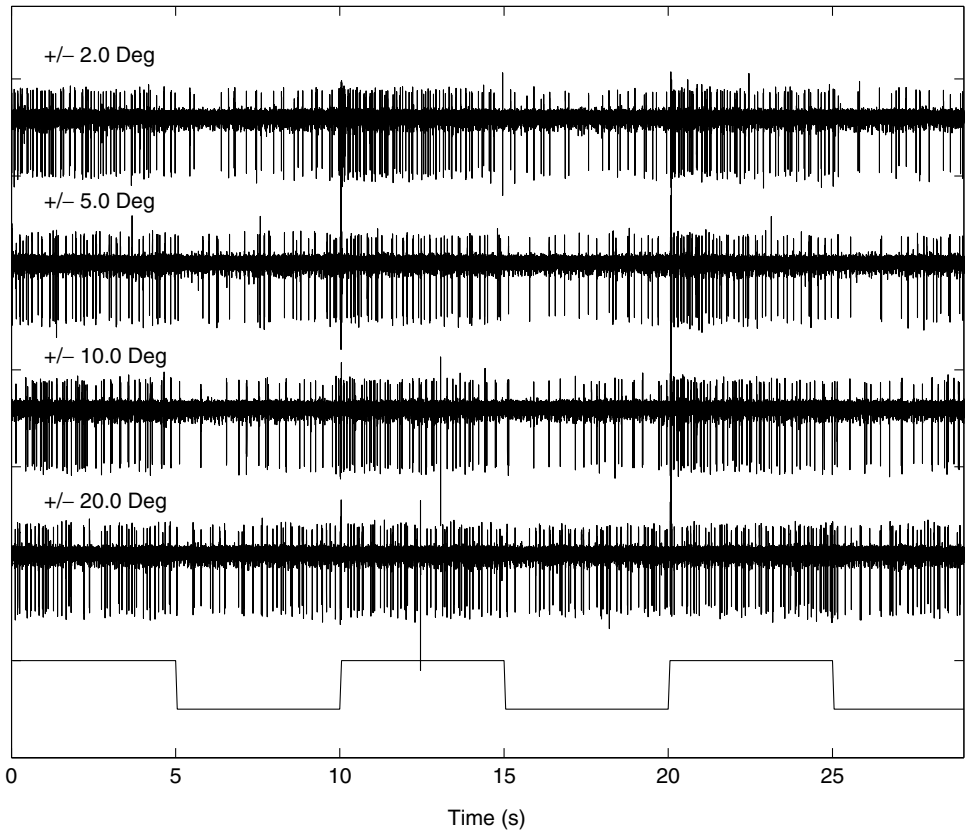

Figure 12. HU motoneuron responses to stepwise displacements of an illuminated stripe subtending 2.8°. The apparent motion crosses the dorsal midline (0°) between the dorso-posterior quadrant (e.g. −2.0°) and the dorso-anterior quadrant (+2.0°). The bottom trace indicates the timing of stimulus displacements.

neuromuscular groups in addition to those studied here. Furthermore, because it is possible that some sensory stimuli coactivate antagonist motoneurons, the activity of one neuron during preferred-direction motion may have little behavioral consequence. This is reflected in the fact that it was the DSI that most closely resembled the behavior, but we cannot rule out the possible behavioral effects of asymmetries between the antagonist neuromuscular groups. These considerations suggest the activity of the HU and HD motoneurons are necessary for the expression of the pitch compensation ocular reflex but they do not establish the sufficient conditions for behavior.

As for the relationship between impulse train parameters and behavior we employed two strategies. First we considered the correlation between stimulus-dependent variations in directional selectivity (derived from the difference in preferred and null mean firing rates) and the gain of the eye rotation. These correlations reflect the relationship between motoneuron impulse rate and muscle contraction and the degree of symmetry between the opposing muscle groups. Previous studies (Wiersma, 1961; Evoy et al., 1967) have shown that in crustacean muscle fibers both the discharge pattern and the correlations between converging neurons influence the contractile response. A linear relationship between motoneuron rate and behavioral gain may actually mask several nonlinear functions with opposing effects (Fuhrmann et al., 2001). Nevertheless, the DSI, computed from mean rates is a strong predictor of reflex gain.

The information theoretic metric is complementary to the correlation analysis which is explicitly linear and assumes a mean rate code. The K-L analysis makes no assumptions regarding the linearity of the stimulus-response relationship. The information theoretic distances between responses to different stimuli vary along each stimulus dimension in a manner commensurate with the requirements of the behavior (Table 1). The K-L distances also indicate that the mean

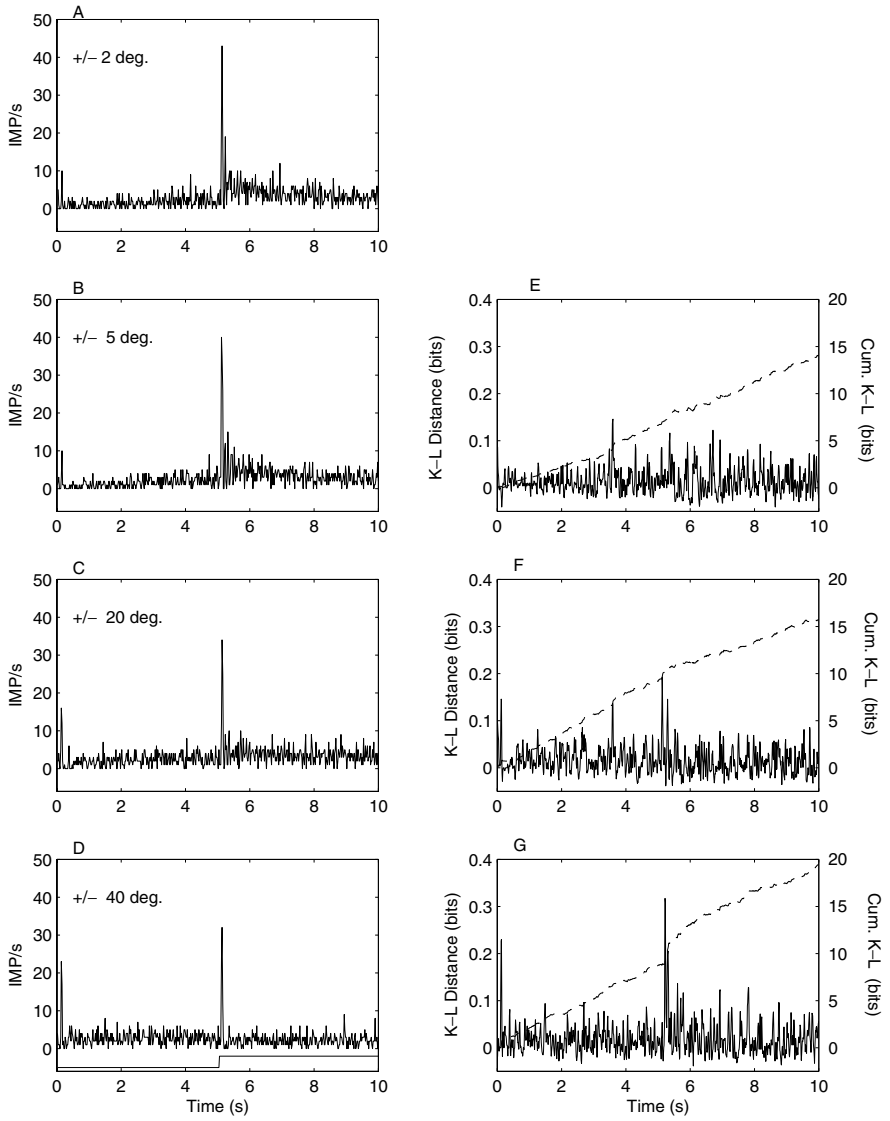

Figure 13. The time course and K-L distances of HU motoneuron responses to varied stepwise displacements of illuminated stripe. (A–D) The PSTs of responses of the same cell shown in Fig. 12 to displacements at indicated angles relative to the dorsal midline of visual space. Stimulus time course is shown in the lower trace in Panel D. $N = 20$ responses per histogram, 20 ms bin width. (E–G) Instantaneous (solid lines) and cumulative (broken lines) K-L distance as a function of time for varied step displacements compared to the response at $\pm 2^\circ$. Each set of functions is based upon a comparison of the response in the adjacent panel (B–D) to the response at $\pm 2^\circ$ reference condition (panel A).

rate makes a substantial contribution to information coding in the responses to global visual motion. The responses to step displacements provide evidence for K-L distances related to the temporal structure of the response.

In the visual cortex, Optican and Richmond (1987), used principle component analysis to show that several features of the impulse train independently encode aspects of transient visual stimuli. Transient responses of cortical visual neurons exhibit bimodal ISI distributions associated with variations in mean impulse rate (Reich et al., 2000) as do crayfish optomotor neurons. In the cortex, the shortest ISIs give rise to the largest information theoretic distances and there are significant differences in the information theoretic distances estimated from ISIs and mean rate (Victor and Purpura,1996; Reich et al., 2000). In crustacean motoneurons variations in impulse rate and ISI

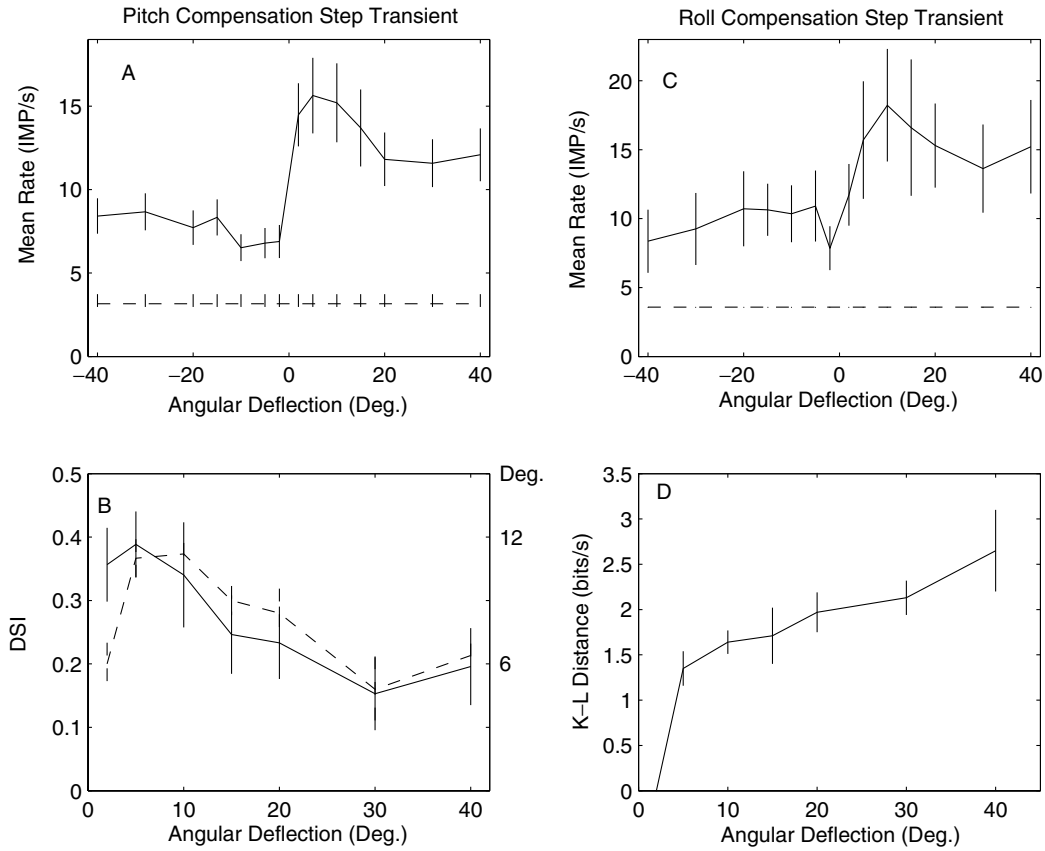

Figure 14. Population average transient rates and DSI for stepwise displacements of illuminated bar. (A) Pitch compensation motoneuron peak rates versus location of 2.8° illuminated bar at end of displacement. Dashed line is average background firing rate. $N = 19$. Vertical bars are ±1.0 S.E. (B) DSI for data in panel A. Broken line is eyestalk deflection for the identical stimuli referenced to the right hand ordinate (from Miller et al., 2002). (C) As in A for roll compensation motoneurons responding to displacement of a 30° wide stripe, $n = 10$. (D) Average K-L distances of pitch compensation motoneurons for 1.0 s of response following displacement of bar and referenced to ± 2.0° displacement. $N = 10$. Vertical lines, ±1.0 S.E.

distribution are highly correlated and are coupled by mechanisms intrinsic to the motoneuron (Kirk and Glantz, 1981). Thus it is not clear if the motoneuron's ISI can have a coding function independent of mean rate. The inference that mean rate is a principle factor in information coding in optomotor neurons is consistent with recent studies of visual cortical neurons (Tovée et al., 1993; Oram et al., 1999) which reach a similar conclusion based upon mutual information computations.

The properties of the K-L distance are also relevant to the third issue we consider, i.e. ensemble coding. When motoneurons are considered two at a time the following picture emerges. The synergists invariably fire in phase with one another (with respect to the direction of grating motion) but the antagonists fire in antiphase. For almost any pair of synergists one of the two neurons is substantially more responsive (in terms of mean impulse rate) than the other and this asymmetry is independent of the stimulus dimension. The joint K-L distances for a pair of antagonists or synergists is somewhat less (83 to 91%) than the sum of the two K-L distances measured separately. This discrepancy is not surprising. If a population K-L distance could increase indefinitely with population size, eventually the output K-L distance would exceed the input distance which is contrary to the Data Processing Theorem (Cover and Thomas, 1991; Johnson et al., 2001). A substantial proportion of the synergists are coupled by excitatory synapses. The crosscorrelograms indicate that for any pair of coupled neurons up to 50% of the object train impulses may occur at 2–10 ms after a reference train impulse. But these correlations appear to have only a small (10%) influence on information

coding (e.g. the joint K-L distances). Because correlated impulses can enhance motor responses (Evoy et al., 1967) in crayfish and postsynaptic impulse generation (Lindsey, 1982; Usrey and Reid, 1999) in crayfish and in other systems it is possible that there may be an inconsistency between the informational content and the behavioral efficacy of the synchronized response. In other systems such as the locust olfactory system, there is good evidence that synchronization among ensemble elements plays an important role in information transmission (Laurent, 1996; MacLeod et al., 1998).

We can also use the Data Processing Theorem to estimate whether a given population is sufficient to produce a behavior. In general we found that the K-L distances associated with any stimulus dimension were larger for the behavioral eye rotation response (Miller et al., 2002) than for single motoneurons (Table 1) but generally less than or equal to the joint K-L distance of 2 to 5 neurons taken simultaneously.

The spatial frequency data is the most important in this context because the underlying functions (gain or directional selectivity) were robust and we obtained the largest data sets for this function in both the neuronal and behavioral studies. At a stimulus amplitude of $\pm 10^\circ$ the K-L distance per 2-fold change in spatial frequency (i.e. per octave) is only marginally greater in the reflex than in the discharge of a single motoneuron. It is possible that the discharge of one motoneuron contains all of the information required by the behavior in this circumstance. At $\pm 45^\circ$, all the K-L distances are larger than at $\pm 10^\circ$ but the K-L distances of the reflex are more than twice that of the individual motoneurons. Consequently, behavioral discrimination requires the summed information content of 2 or 3 motoneuron responses in this instance. For the 12 comparisons in Table 1, the response of one motoneuron satisfies the informational requirements of the behavior in three instances (spatial frequency and contrast at $\pm 10^\circ$) but the summed K-L distances of 2 to 5 motoneurons appears to be necessary in eight instances. This result has the important implication that the behaviorally relevant information signal is generally distributed across the motoneuron population.

Aspects of impulse train coding can be further specified through an analysis of the temporal encoding window, i.e. the limiting time interval in which a message is contained (Theunissen and Miller, 1995). The duration of this window constrains the possible coding strategies (e.g. the number of impulses) employed by the system. For behavioral step responses the modal time to peak response was 600 ms (Miller et al., 2002). By 600 ms both the direction and extent of eye movement are expressed. Because there are mechanical delays in muscle contraction it is likely that the motoneuron response is formed in 500 ms or less. The time to peak of a motoneuron step response is about 175 ms (as in Table 2) but the K-L distance distinguishing responses to steps in opposite directions (1.0 bit) requires 380 to 470 ms in a single motoneuron. During this K-L latency period each motoneuron generates 2 to 3 impulses in addition to the 1.2 impulses associated with the background discharge. When the same analysis is applied to the responses to grating motion, the durations of the encoding windows are longer (0.6 to 1.0 s) but the number of stimulus-elicited impulses within these windows is about the same. Both the necessary duration of the encoding window and the number of spikes/neuron in

Table 2. Response latencies and times for directional responses to exhibit a 1.0 bit K-L distance.

Stimulus	Neuron	N	Response latency[a] (ms)	K-L latency[b] (ms)	Added impulses[c]
Step	HU Mn	45	173 ± 9	381 ± 24	1.91 ± 0.93
Step	HD Mn	34	165 ± 10	466 ± 28	2.38 ± 1.29
Step	SD Mn	45	184 ± 8	462 ± 34	1.53 ± 0.72
Grating (16°/s)	HD Mn	27	192 ± 17	614 ± 63	2.51 ± 0.42
Grating (3.2°/s)	HD Mn	36	333 ± 55	923 ± 95	1.81 ± 0.30

[a]Latencies for step response equal the time from stimulus onset to the peak of the PST. Latencies for grating responses indicate the time required from onset of stimulus motion for the response to preferred-direction motion to exceed 2.0 S.D. above the mean response to null-direction motion.

[b]K-L latencies represent the time required from stimulus onset for the K-L distance between preferred and null direction responses to exceed 1.0 bit.

[c]Added impulses are the number of spikes per Mn above the background discharge from stimulus onset to the post-stimulus time required to achieve 1.0 bit in the directional K-L distance.

the window will be smaller for ensembles compared to single cells.

Conclusions

Although the DSI of optomotor neuron responses is correlated to the gain of the pitch compensation reflex (for four stimulus dimensions), the stimulus information in a single motoneuron response is in general not sufficient to support the stimulus discriminations exhibited by the reflex. Information theoretic analysis reveals that the behaviorally relevant information is generally conveyed by an ensemble of 2 to 5 neurons. Synapses between motoneurons can produce strong correlations in the impulse times of coactivated cells but these correlations make only a small contribution to information transmission. Rather, the motoneuron mean impulse rate appears to be a major determinant of the information transmitted by the discharge. The temporal encoding window for the discrimination of the direction of stimulus motion by a single neuron is less than 300 ms beyond the response latency for the step response and contains no more than 3 impulses. For global motion the encoding window occupies up to a second but the number of impulses is similar.

Acknowledgments

Supported by grants from the National Institutes of Health MH60861-01 and the National Science Foundation, CCR-0105558.

References

Burrows M, Horridge GA (1968) Motoneurone discharges to the eyecup muscles of the crab, *Carcinus*, during optokinetic movements. J. Exp. Biol. 49: 251–267.

Cover TM, Thomas JA (1991) Elements of information theory. John Wiley & Sons, Inc.

deCharms RC, Zador A (2000) Neural representation and the neural code. Annual Rev. Neurosci. 23: 613–647.

Egelhaaf M, Borst A, Reichardt W (1989) Computational structure of a biological motion detection system as revealed by local detector analysis in the fly's nervous system. J. Opt. Soc. Am. A 6: 1070–1087.

Evoy WH, Kennedy D, Wilson DM (1967) Discharge patterns of neurons supplying tonic abdominal flexor muscles in the crayfish. J. Exp. Biol. 46: 393–411.

Fuhrmann G, Segev I, Markram H, Tsodyks M (2002) Coding of temporal information by activity dependent synapses. J. Neurophysiol. 87: 140–148.

Gillary HL, Kennedy D (1969) Neuromuscular effects of impulse pattern in a crustacean motoneuron. J. Neurophysiol. 32: 607–612.

Glantz RM, Nudelman HB (1976) Sustained, synchronous oscillations in discharge of sustaining fibers of crayfish optic nerve. J. Neurophysiol. 39: 1257–1271.

Glantz RM, Nudelman HB, Waldorp B (1984) Linear integration of convergent visual inputs in an oculomotor reflex pathway. J. Neurophysiol. 52: 1213–1225.

Hisada M, Higuchi T (1973) Basic response pattern and classification of oculomotor nerve in the crayfish, Procambarus clarkii. J. Fac. Sci. Hokkaido Univ. Series VI Zool. 18: 481–494.

Johnson DH (2002) Four top reasons mutual information does not quantify neural information processing. Computational Neuroscience '02. Chicago Ill. July, 2002.

Johnson DH, Gruner CM, Baggerly K, Seshagiri C (2001) Information-theoretic analysis of neural coding. J. Computational Neuroscience 10: 47–69.

Kirk MD, Glantz RM (1981) Impulse pattern generation in a crayfish abdominal postural motoneuron. J. Comp. Physiol. 141: 183–196.

Laurent G (1996) Dynamical representation of odors by oscillating and evolving neural assemblies. Trends in Neurosci. 19: 489–496.

Lindsey BG (1982) Measurement and dissociation of action potentials in concurrently active parallel channels on motoneuron activity in crayfish. J. Neurophysiol. 47: 1160–1173.

MacLeod K, Bäcker A, Laurent G (1998) Who reads temporal information contained across synchronized and oscillatory spike trains? Nature 395: 693–698.

Mellon DeF (1977) The anatomy and motor nerve distribution of the eye muscles in the crayfish. J. Comp. Physiol. 121: 349–366.

Mellon DeF, Lorton ED (1977) Reflex actions in the functional divisions in the crayfish oculomotor system. J. Comp. Physiol. 121: 367–380.

Mulloney B, Selverston AI (1974) Organization of the stomatogastric ganglion of the spiny lobster. J. Comp. Physiol. 91: 1–32.

Miller CS, Johnson DH, Schroeter JP, Myint L, Glantz RM (2002) Visual signals in an optomotor reflex: Systems and information theoretic analysis. J. Comput. Neurosci. 13: 5–21.

Neil DM, Schöne H, Scapini F, Miyan JA (1983) Optokinetic responses, visual adaptation and multisensory control of eye movements in the spiny lobster, Palinurus vulgaris. J. Exp. Biol. 107: 349–366.

Optican LM, Richmond BJ (1987) Temporal encoding of two-dimensional patterns by single units in a primate inferior temporal cortex. III Information, theoretic analysis. J. Neurophysiol. 57: 162–178.

Oram MW, Wiener MC, Lestienne R, Richmond BJ (1999) Stochastic nature of precisely timed spike patterns in visual system neuronal responses. J. Neurophysiol. 81: 3021–3033.

Reich DS, Mechler F, Purpura KP, Victor JD (2000) Interspike intervals, receptive fields and information coding in primary visual cortex. J. Neurosci. 20: 1964–1975.

Robinson CA, Nunnemacher RF (1966) The musculature of the eyestalk of the crayfish, Orconectes Virilis. Crustaceana 11: 77–82.

Silvey GE, Sandeman DC (1976) Integration between statocyst sensory neurons and oculomotor neurons in the crab, Scylla serrata. III. The sensory to motor synapse. J. Comp. Physiol. 108: 53–65.

Smith DO (1974) Autogenic production of paired pulses by the opener excitor neuron of the crayfish claw. Brain Res. 70: 356–360.

Tatton WG, Sokolove PG (1975) Analysis of postural motoneuron activity in crayfish abdomen. II Coordination by excitatory and inhibitory connections between motoneurons. J. Neurophysiol. 38: 332–346.

Theunissen FE, Miller JP (1991) Representation of sensory information in the cricket cercal sensory system. II Information theoretic calculation of system accuracy and optimal tuning-curve widths of four primary interneurons. J. Neurophysiol. 66: 1690–1703.

Theunissen F, Miller JP (1995) Temporal coding in nervous systems: A rigorous definition. J. Comput. Neurosci. 2: 149–162.

Tovée MJ, Rolls ET, Treves A, Bellis RP (1993) Information encoding and the responses of single neurons in the primate temporal visual cortex. J. Neurophysiol. 70: 640–654.

Usrey WM, Reid RC (1999) Synchronous activity in the visual system. Ann. Rev. Physiol. 61: 435–456.

Victor JD, Purpura KP (1996) Nature and precision of temporal coding in visual cortex: A metric-space analysis. J. Neurophysiol. 76: 1310–1326.

Wiens TJ, Gerstein GL (1975) Cross connections among crayfish claw efferents. J. Neurophysiol. 38: 909–921.

Wiersma CAG (1961) The neuromuscular system. In: TH Waterman, ed. The Physiology of Crustacea. Vol. 2. Academic Press, New York. pp. 191–240.

Wiersma CAG, Oberjat T (1968) The selective responsiveness of various crayfish oculomotor fibers to sensory stimuli. Comp. Biochem. and Physiol. 26: 1–16.

York B, Wiersma CAG (1975) Visual processing in the rock lobster. Prog. Neurobiol. 5: 127–166.